Information Sciences Letters

Volume 10
Issue 3 *Sep. 2021*

Article 11

2021

Design and Mathematical Modeling of CMOS Compatible - MEMS Microhotplate

Wafaa Elsayed Elbasty
Department of Electrical and Electronics Engineering, Universiti Teknologi PETRONAS, Perak, Malaysia, illani.nawi@utp.edu.my

Illani Bt Md Nawi
Department of Electrical and Electronics Engineering, Universiti Teknologi PETRONAS, Perak, Malaysia, illani.nawi@utp.edu.my

Mohd Haris Md Khir
Department of Electrical and Electronics Engineering, Universiti Teknologi PETRONAS, Perak, Malaysia, illani.nawi@utp.edu.my

Abdelaziz Yousif Ahmed
Department of Electronic Engineering, University of Gezira, Wad Madani, Sudan, illani.nawi@utp.edu.my

Information Sciences Letters
An International Journal

http://dx.doi.org/10.18576/isl/100312

Design and Mathematical Modeling of CMOS Compatible - MEMS Microhotplate

Wafaa Elsayed Elbasty[1], *Illani Bt Md Nawi*[1,*], *Mohd Haris Md Khir*[1] *and Abdelaziz Yousif Ahmed* [2]

[1]Department of Electrical and Electronics Engineering, Universiti Teknologi PETRONAS, Perak, Malaysia
[2]Department of Electronic Engineering, University of Gezira, Wad Madani, Sudan

Received:21 Feb. 2021, Revised: 22 Mar. 2021, Accepted: 24 Apr. 2021.
Published online:1 Sep. 2021.

Abstract: Current Microhotplates have large power consumptions, temperature uniformity problems, and are highly priced; additionally, special stages are required to be integrated with ICs. The modeling and design of a MEMS Microhotplate (MHP) using standard 0.18 µm IP4M CMOS process technology is discussed in this paper. The designed MHP is intended to achieve good temperature uniformity while dissipating little power. The MHP microbridges lengths are varied from 80 µm to 120 µm whereas the MHP microbridges widths are varied from 5 µm to 25 µm. The effect of the length and width are studied and three different lengths of micro heater 15560 µm, 24360 µm, 35160 µm, and 5 µm width were studied. The optimized design with microbridges of 100 µm length and 25 µm width and a heater length of 15560 µm is selected. The power dissipation and operating temperature were measured using mathematical modeling and actuation voltages ranging from 0.2 V to 1 V. The modeling estimates MHP power dissipation ranging from 0.264 mW to 3.181 mW at operating temperatures ranging from 11.12 oC to 277.92 oC.
Keywords: MHP, MEMS, and CMOS technology.

1 Introduction

Thermal sensors, gas detectors, microscopic thermal infrared emitters, microthrusters, display packaging, micro/nano-fluidics, and microcalorimeters are only a few of the applications for microhotplate. Microhotplates in a microcalorimeter aid in achieving a small sample volume, fast response, and high sensitivity [1]. Chemical sensors are commonly used by microhotplates to develop the sensor response by enhancing chemical reactions between the sensor film and the gas species [2]. MHP is a thermally isolated process designed using micro-technology processes. The MHP layers consist of a substrate, a membrane, a heating element, a heat dispenser, and a temperature sensor to measure the temperature of the MHP. Two or three electrodes are used on the upper layer to measure the resistance or impedance of the sensing material. The reliability of the microhotplate depends mainly on choice of heating and membrane materials, geometry of the heater, form of membrane (close or open) [3]. The development of MHP is closely coupled with novel nanotechnology manufacturing strategies as well as micro-deposition and micro-structuring. Microelectromechanical system (MEMS) has been used to develop and design microhotplate, where

MEMS is a state-of-the-art cross-field technology that combines microelectronics with micromachining technology to integrate microcomponents, microsensors and micro actuators, signal processing and control circuits, etc. MEMS is now popular in the daily lives [4]. This technology has been used to develop and produce MHPs with high operating temperatures, low power consumption and good uniformity temperature. However, most of the device's fabrication is costly and not easily integrated with IC. Thus, the demand for continuous miniaturization and reduced power consumption drives the research of Metal Oxide (MOX) gas sensors towards the direct integration of the MEMS sensing structure with the integrated circuits for signal conditioning circuits [5]. This integration is traditionally achieved with a multi-chip approach in which the sensor and circuits are designed and manufactured on separate chips.

Multi-chip integration allows the MEMS sensor and complementary metal oxide semiconductor (CMOS) circuits to be optimized independently. It also offers more flexibility in design and manufacturing so that less time for production is required. However, additional expenses are incurred in conjunction with complicated packaging and wire bonds. The parasitic element of the interconnection provides rise to additional noise [6].

*Corresponding author e-mail: illani.nawi@utp.edu.my

A more advanced way to incorporate CMOS-MEMS is the monolithic approach, where sensors and circuits are built and fabricated on a single substrate. Monolithic integration improves the efficiency of the sensor by reducing its scale, power consumption and noise [6]. High manufacturing costs and a long development period can be offset by a reduction packaging costs for large-volume production. The challenge of the monolithic approach is the limitation of materials available for the CMOS process. The performance of a microhotplate is primarily determined by the choice of heating and membrane materials, heater geometry, membrane type (close or open), and fabrication technique. Different researchers have used different heating materials.

Thus, Li et al. [7] designed and fabricated CMOS-compatible MHP gas sensor with a standard industrial CMOS technology (0.5 μm MPW). The tungsten plug between the first and second metal layers is built as a zigzag resistor heater inserted in the centre of the membrane. Aluminum is used as sensing film electrodes. Pt / Ti layer of 200 nm was used to resolve the oxidation of the aluminum electrodes issue. The device had low power consumption (19 mW) and a rapid thermal response time (8 ms) for heating up to 300 ºC. The devices heater could operate dependably with negligible shift in the resistance (<0.3%) at an operation temperature of 300 ºC under constant heating mode for 336 h. The tungsten heater was acted as thermometer to measure the operated temperature in the device.

Liao et al. [8], the manufacturing and characterization of an ethanol microsensor equipped with a heater were studied and investigated. The ethanol sensor is produced using a commercial CMOS process of 0.18 μm. The sensor contains of a sensitive film (ZnO), a polysilicon heater and interdigital electrodes (Aluminum and Tungsten).

In order to measure the characteristics of the heater in the ethanol sensor, a power supply, an infrared thermometer and an LCR meter were used. The power supply supplied the voltage to heater, and the infrared thermometer detected the temperature of the heater. The results showed that the heater produced a temperature of 350 °C when a power of 19.5 mW was applied.

Yang and Dai [9] designed and manufactured an ethanol microsensor integrated with an on-a-chip readout circuit using CMOS-MEMS technique. The ethanol sensor consists of a heater, a sensitive film, and interdigitated electrodes. The sensitive film was operating temperature of 220 °C. The material of the interdigitated electrodes is the aluminum metal of the CMOS process. The heater material is made of polysilicon. The heater is designed as a winding line used to supply the working temperature to the sensitive film. The integrated ethanol sensor chip was fabricated using the commercial 0.18 μm CMOS process of the Taiwan Semiconductor Manufacturing Company (TSMC, Taipei, Taiwan). The heater supplied the sensor with a working temperature of 220 °C and the power consumption of 73mW.

The development of the microhotplate is extensive; however, several of the current MHP have high-power consumption, uniformity temperature issue, high fabrication cost and cannot be easily integrate with IC. Additionally, many materials have been used for the design of MHP like platinum and gold. Despite they are ideally suited to microheaters with a wide temperature range, accuracy and stability, platinum and gold are costly and not compatible with CMOS technology [10].

The aim of this paper is to design microhotplate-based CMOS-MEMS using 0.18 μm 1P4M CMOS technology. The CMOS process used consists of 1 polysilicon layer, four metal layers, and five dielectric layers. All metal layers are made of aluminum (Al), the dielectric layers are silicon dioxide (SiO_2). Then, an appropriate mathematical modeling will be done on the parameters of the MEMS-MHP in order to optimize a CMOS-MEMS MHP.

2 The Micro Hotplate Design

The CMOS-MEMS Microhotplate (MHP) will be mathematically designed based on the standard 0.18 μm IP4M CMOS process technology. The device structure consists of four metals, one poly-Si and five dielectric layers. Figure 1 shows the schematic of the cross-sectional view of CMOS –MEMS MHP layers, where the aluminum is chosen because of low cost, low corrosion, and thermal stability. Thus, aluminum (Al) is the material that all four metal layers are made of and the five dielectric layers are made of silicon dioxide (SiO2).

M1 and M3 will be used as heat distributor to get a good uniformity temperature. M2 will be used as heater together with the temperature sensor where, sensor deposited above the microheater on the same layer. Heater is being designed using meander form. M4 is going to be used as interdigitated electrode (IDE), to overcome the problem of aluminum oxidation. Silicon nitride is to be used for passivation layer over the electrode. Forming the microheater and IDE in different layers will improve the temperature uniformity as compared to the same layer integrated. The device should have a good mechanical stability; thus, suspended membrane type with four arms will be used. Figure 2 shows the MHP top view schematic design while, Tables 1 and 2 present all material properties of layers and specifications of the layers materials at the active area of the MHP used in the CMOS -MEMS microhotplate structure.

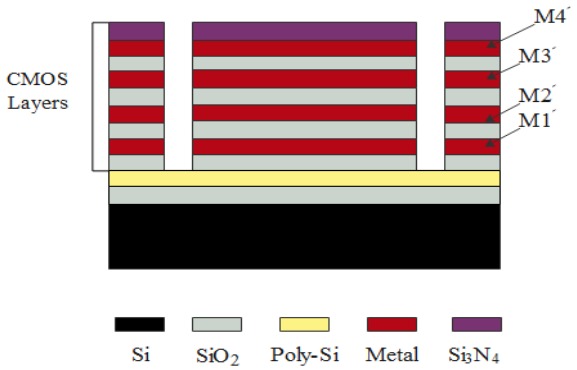

Fig. 1: Schematic of the cross-sectional view of CMOS-MEMS MHP

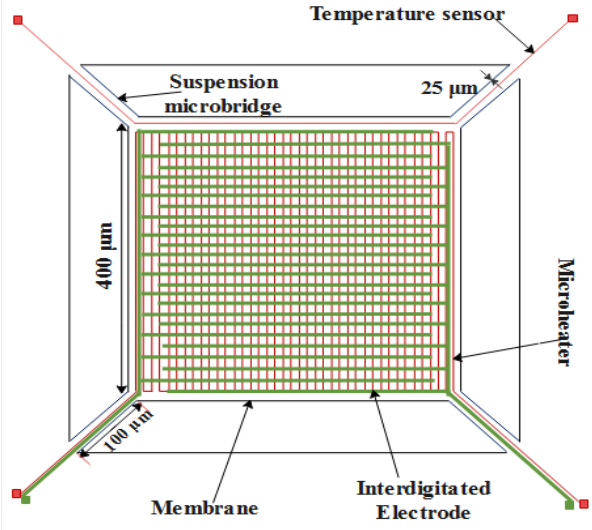

Fig. 2: Schematic top view of MHP design

Table 1: Material properties of layers used in the cmos - mems microhotplate structure

Materials	Si	SiO_2	Poly-Si	Al	Si_3N_4
Young's modulus (GPa)	130	70	160	72	290
Poisson ratio	0.25	0.17	0.15	0.33	0.27
Density (kg/m^3)	2300	2648	2331	2700	2900
Specific heat capacity (J/kg.K)	710	730	100	900	-
Thermal conductivity (W/K.m)	150	1.4	34	240	29
Coeff. of thermal expansion	2.33	0.55	2.33	23.2	3.3
Melting point (°C)	1400	1700	414	660	1480

Table 2: Specifications of the layers materials at the active area of the MHP

Layers	Thickness µm	Width µm	length µm
Si	300	450	450
Sio2	0.56	450	450
Poly	0.56	450	450
Heater distributor plate(metal 1&3)	0.56	400	400
Temperature sensor	0.56	5	800
Interdigited electrode	0.56	5	11600
Passivation layer (Si3N4)	0.56	450	450

Aluminum (Al) was used as the material of the microheater, temperature sensor and IDE. The microheater shape is in meander form with length 15560 µm together with the temperature sensor with length of 800 µm and width of 5 µm is above the microheater on the same layer shown in Figure 3. IDE (Al) with length 11600 µm and width 5 µm as shown in Figure 4.

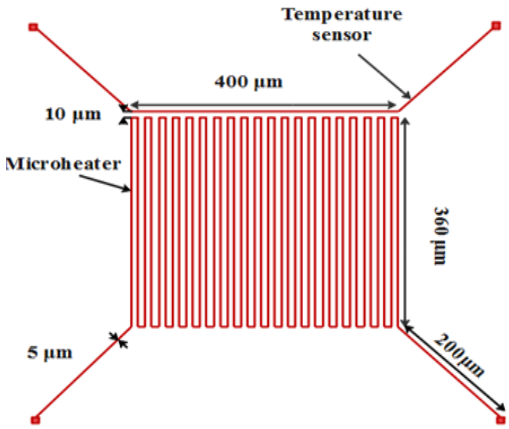

Fig. 3: Schematic of micro heater and temperature sensor design.

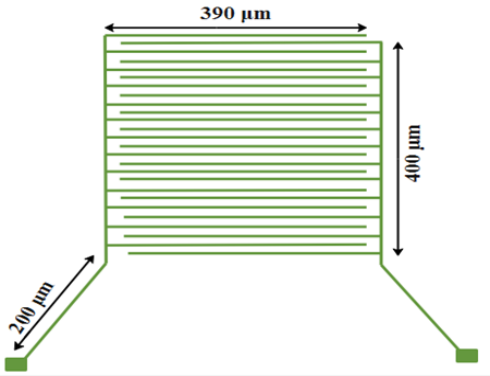

Fig. 4: Schematic of interdigitated electrodes.

3 Mathematical Modeling of the Microhotplate

The heat loss through conduction is measured, while the heat losses through radiation and convection are ignored because the amount of heat loss through them is usually very small in comparison to the heat loss from conduction. Conduction occurs when thermal energy is moved from a high-temperature region to a low-temperature area. Conduction happens around the microbridges in the MHP structure, the power dissipation (P_{disp}) can be calculated by (1), while the power conduction through the membrane can be calculated by (2 or 3) [11].

$$P_{disp} = P_{conduction} \quad (1)$$

$$P_{conduction} = 4KA\frac{dT}{dx} \quad (2)$$

K is thermal conductivity of the material in W/m.K, A is cross sectional area normal to the direction of heat flow, in m^2, T is the temperature, and x is the direction of the heat flow.

$$P_{conduction} = \frac{\Delta T}{R_{th}} \quad (3)$$

The effect of length variation from 80 µm to 12 µm and width of the microbridges from 5 µm to 25 µm is investigated in this section by using thermal resistances, R_{th} and thermal capacitances, C_{th}. The thermal resistances, R_{th} are defined by using (4).

$$R_{th} = \frac{l}{KA} \quad (4)$$

$$\frac{1}{R_{th(1bridge)}} = \frac{1}{R_{th(poly-si)}} + \frac{5}{R_{th(sio_2)}} \quad (5)$$

$$R_{th(4bridge)} = \frac{R_{th(1bridge)}}{4} \quad (6)$$

The thermal capacitance, C_{th} can be calculated by using (7) while the total C_{th} can be defined using (8)

$$C_{th} = \rho v c \quad (7)$$

$$C_{th\,(1bridge)} = C_{th\,(poly-si)} + 5C_{th\,(sio_2)} \quad (8)$$

$$C_{th\,(4bridge)} = 4C_{th\,(1bridge)} \quad (9)$$

where ρ is the density, v is the volume of the layer, and c is the specific heat capacity of the layer.
The response time at which the temperature of the microheater rises or falls can be calculated by (10).

$$\tau = C_{th(4bridges)}R_{th(4bridges)} \quad (10)$$

After that, three different lengths of micro heater 15560 µm, 24360 µm, 35160 µm, and 5 µm width with the effect of length variation from 80 µm to 120 µm and constant width 25µm of microbridges together with an applied voltage from 0.2V to 1V were studied.
Firstly, the electrical resistance of microheater R_o will be determined using (11) [11],

$$R_o = \rho\frac{L}{w.t} \quad (11)$$

where ρ is the electrical resistivity of Al is equal to 2.82×10^{-8}, L, w, t are the length, width and thickness of the Al wires, respectively.

In MHP, it is critical to understand the amount of voltage needed to raise the temperature to the desired temperature. A voltage is applied through the microheater terminals to produce the temperature. The relationship between temperature and applied voltage is represented as follows (12):

$$\Delta T = \frac{V^2}{R_o}R_{th(4bridge)} \quad (12)$$

where ΔT is the difference in the operating temperature, R_o is the electrical resistance at the ambient temperature, and V is the microheater voltage while $R_{th(4bridges)}$ is the total thermal resistance of the MHP microbridges.
The resistance of the microheater as a function of temperatures can be determined as in (13),

$$R(T) = R_O[1 + \alpha\Delta T] \quad (13)$$

where $R(T)$ is the resistance at temperature T. For Al, the standard value of α is 0.0039 K^{-1} [11].
After the resistance of the microheater is determined, the power consumption ($P_{consumption}$) of the microheater can be calculated using (14).

$$P_{consumption} = \frac{V^2}{R} \quad (14)$$

The microheater current density can be obtained by using (15),

$$J = \frac{V/R}{dw} \quad (15)$$

where J is the current density, R is the microheater resistance, d and w is the thickness and width of the microheater, respectively [11].

4 Results and Discussions

In this section the results determined by the theoretical modeling is presented. The thermal resistance (R_{th}) and thermal capacitance (C_{th}) of the microbridges have been calculated and analyzed in order to determine the actual power dissipation by the conduction. Furthermore, the thermal time constant (τ), electrical resistance (R_o), relationship between operating temperature (T) and applied voltage (V) as well as power dissipation ($P_{dissipation}$) and current density (J) had also been calculated to determine the characteristics of the MHP.

A. Thermal Resistance, Thermal Capacitance, and Thermal Time Constant.

The effect of the variation in the length and width of microbridges from 80 µm to120 µm and from 5 µm to 25 µm, respectively on the thermal resistance and thermal capacitance was investigated. A significant increase can be seen in the thermal resistance as the length of microbridges increases. A remarkable decrease in the thermal resistance has been displayed as the width of microbridges increases. These two observations are presented in Table 3 and Figure 5. Increasing in both width and length of the microbridges led to an increase in the thermal capacitance as presented in Table 4 and Figure 6. Furthermore, the thermal time constant reduces as the width of microbridges increases as presented in Table 5 and Figure 7.

Table 3: Thermal resistance with different lengths and widths of microbridges

Thermal Resistance (10^6 K/W)					
Width (µm)	Length(µm)				
	80	90	100	110	120
5	0.174	0.196	0.218	0.239	0.261
10	0.087	0.098	0.109	0.119	0.131
15	0.058	0.065	0.073	0.079	0.087
20	0.044	0.049	0.054	0.059	0.065
25	0.035	0.039	0.044	0.047	0.052

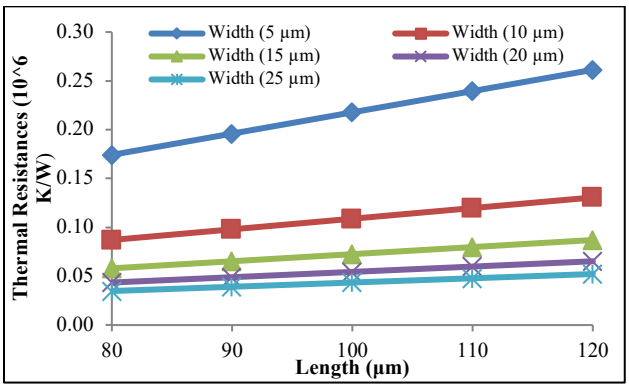

Fig. 5: Thermal resistance with different lengths and widths of microbridges.

Table 4: Thermal capacitance with different lengths and widths of microbridges

Thermal Capacitor (J/K)					
Width (µm)	Length(µm)				
	80	90	100	110	120
5	8.9E-09	9.9E-09	1.1E-08	1.2E-08	1.3E-08
10	1.8E-08	1.2E-08	2.2E-08	2.4E-08	2.7E-08
15	2.7E-08	2.9E-08	3.3E-08	3.7E-08	3.9E-08
20	3.6E-08	3.9E-08	4.4E-08	4.9E-08	5.3E-08
25	4.4E-08	4.9E-08	5.5E-08	6.1E-08	6.7E-08

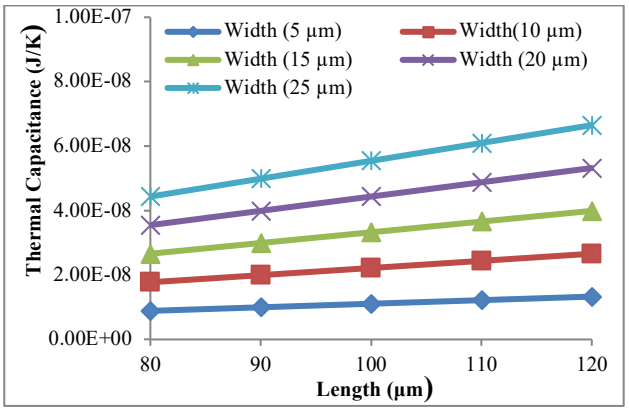

Fig. 6: Thermal capacitance with different lengths and widths of microbridges

Table 5: Thermal time constant with different length and widths of microbridge

Thermal Time (ms)					
Width (µm)	Length(µm)				
	80	90	100	110	120
5	30.9	34	38.6	42.5	46.4
10	15.5	17.4	19.3	21.2	23.2
15	10.3	11.6	12.9	14.2	15.5
20	7.7	8.7	9.7	10.6	11.6
25	6.2	7.0	7.7	8.5	9.3

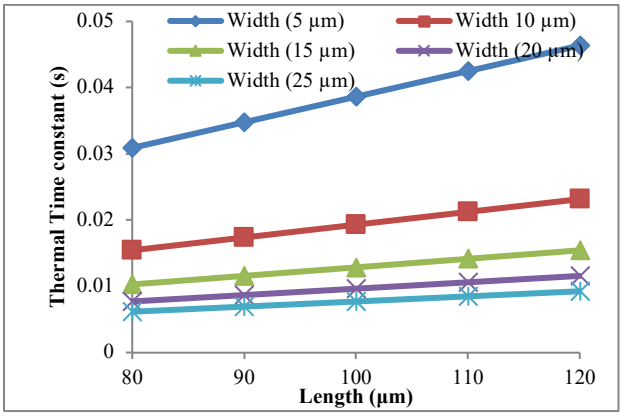

Fig. 7: Thermal time constant of the MHP different lengths and widths of microbridges.

B. Operating Temperature, Electrical Resistance ,Power and Current Density of the heater

The obtained results showed that the length of the microbridges is directly proportional with the electrical resistance as shown in Table 6. In addition, the operating temperature, power, and current density of the MHP were determined at each heaters length.

Table 6: The electrical resistance for the three different heater lengths

Heater length (µm)	R_o (Ω)
15560	156.71
24360	245.34
35160	354.11

i. Operating temperature vs. microbridges lengths.

Generally, increasing the microheater length from 15560 µm to 35160 µm led to a decrease in the operating temperature. On the other hand, the operating temperature increases as the length of microbridges and applying various voltages increases as shown in Tables 7, 8, 9 and Figures 8, 9, 10. The highest operating temperature with the three different heater lengths (333.510 ºC, 213.030 ºC and 147.594 ºC) were recorded at the 120 µm microbridge length and 1 V applied voltage.

Table 7: The operating temperature of heater under different microbridge lengths and applied voltages at 15560 µm microheater length

Voltage (V)	Operating temperature (ºC)				
	Length(µm)				
	80	90	100	110	120
0.2	8.89	10.01	11.12	12.23	13.34
0.4	35.57	40.02	44.47	48.92	53.36
0.6	80.04	90.05	100.05	110.06	120.06
0.8	142.29	160.09	177.87	195.66	213.45
1.00	222.34	250.13	277.92	305.72	333.51

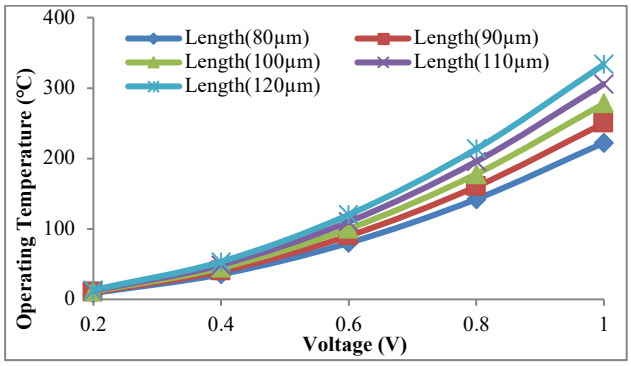

Fig. 8: The operating temperature of heater under different microbridge lengths and applied voltages at 15560 µm microheater length

Table 8: The operating temperature of heater under different microbridge lengths and applied voltages at 24360 µm microheater length

Voltage (V)	Operating temperature (ºC)				
	Length(µm)				
	80	90	100	110	120
0.2	5.68	6.39	7.10	7.81	8.52
0.4	22.72	25.56	28.40	31.24	34.08
0.6	51.12	57.51	63.90	70.29	76.69
0.8	90.89	102.25	113.61	124.97	136.33
1.00	142.02	159.77	177.52	195.27	213.03

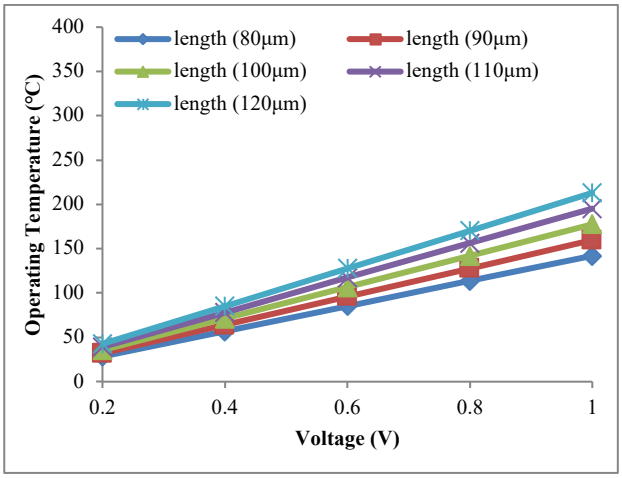

Fig. 9: The operating temperature of heater under different microbridge lengths and applied voltages at 24360 µm microheater length

Table 9: The operating temperature of heater under different microbridge lengths and applied voltages at 35160 µm microheater length

Voltage (V)	Operating temperature (°C)				
	Length(µm)				
	80	90	100	110	120
0.2	3.93	4.42	4.919	5.41	5.90
0.4	15.74	17.71	19.679	21.64	23.61
0.6	35.42	39.85	44.278	48.70	53.13
0.8	62.97	70.84	78.717	86.58	94.46
1.00	98.39	110.69	122.99	135.29	147.59

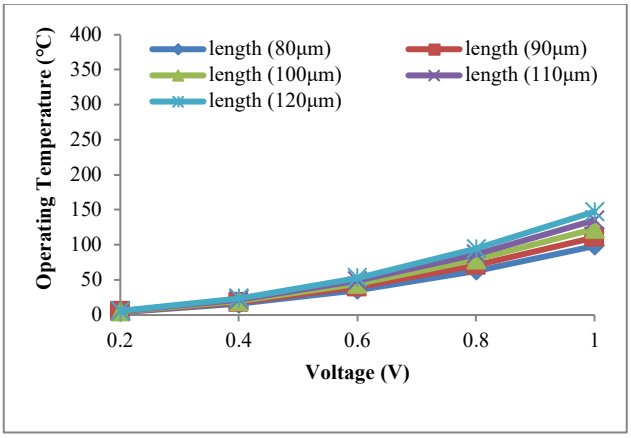

Fig. 10: The operating temperature of heater under different microbridge lengths and applied voltages at 35160 µm microheater length

ii. Power vs. microbridges lengths.

The power consumption has the same trend as operating temperature while increasing the length of the heater as presented in Tables 10, 11, 12 and Figures 11, 12, 13. A slight decrease in the power consumption is expected as the length of microbridges increases. Furthermore, as voltages increases the power consumption increases.

Table 10: Power consumption of MHP under different microbridge lengths and applied voltages at 15560 µm microheater length

Voltage (V)	Power (mW)				
	Length(µm)				
	80	90	100	110	120
0.2	0.27	0.27	0.26	0.26	0.262
0.4	0.96	0.95	0.93	0.92	0.903
0.6	1.86	1.80	1.75	1.70	1.652
0.8	2.77	2.64	2.53	2.42	2.328
1.00	3.57	3.36	3.18	3.02	2.871

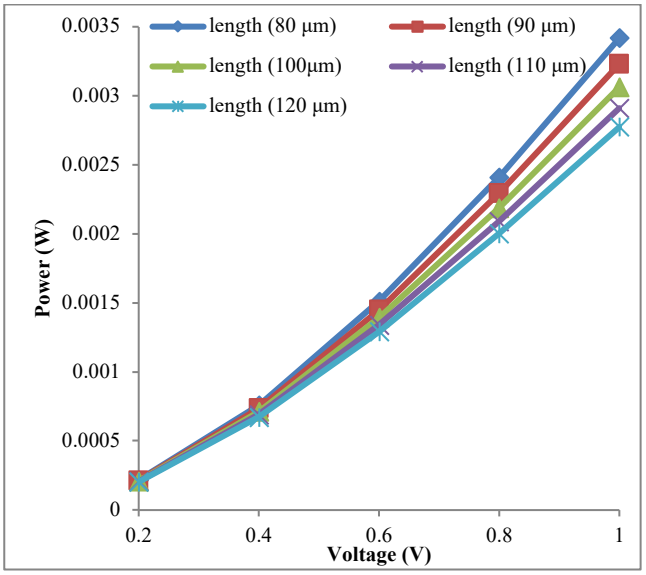

Fig. 11: Power consumption of MHP under different microbridge lengths and applied voltages at 15560 µm microheater length

Table 11: Power consumption of MHP under different microbridge lengths and applied voltages at 24360 µm microheater length

Voltage (V)	Power (mW)				
	Length(µm)				
	80	90	100	110	120
0.2	0.17	0.17	0.17	0.17	0.17
0.4	0.65	0.64	0.631	0.63	0.62
0.6	1.31	1.28	1.253	1.23	1.20
0.8	2.04	1.98	1.911	1.85	1.79
1.00	2.76	2.64	2.525	2.42	2.36

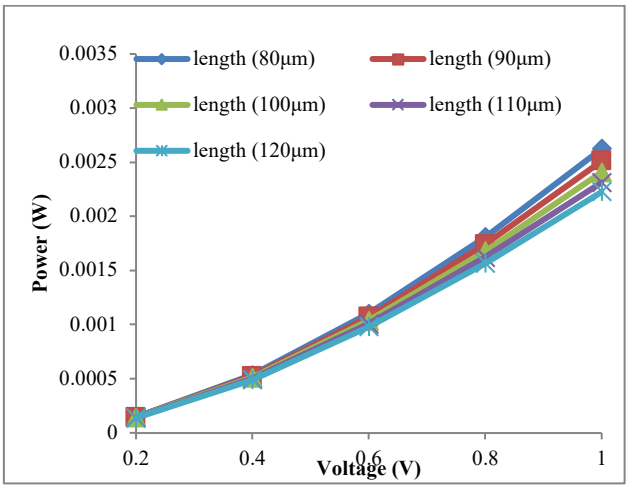

Fig. 12: Power consumption of MHP under different microbridge lengths and applied voltages at 24360 µm microheater length

Table 12: Power consumption of MHP under different microbridge lengths and applied voltages at 35160 µm microheater length

Voltage (V)	Power (mW) Length(µm)				
	80	90	100	110	120
0.2	0.121	0.120	0.120	0.120	0.120
0.4	0.459	0.456	0.452	0.449	0.446
0.6	0.959	0.944	0.929	0.914	0.900
0.8	1.55	1.51	1.47	1.43	1.40
1.00	2.16	2.09	2.01	1.95	1.89

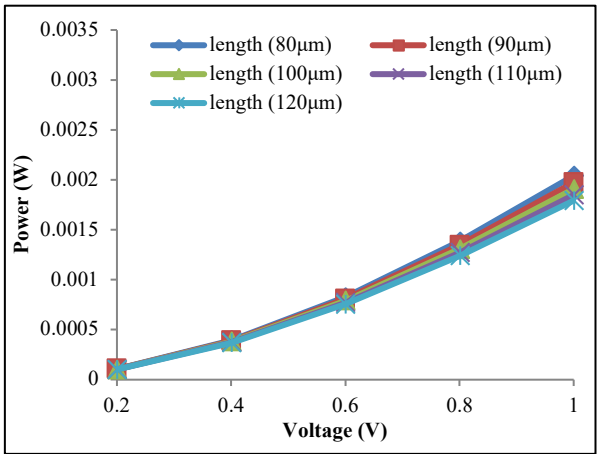

Fig. 13: Power consumption of MHP under different microbridge lengths and applied voltages at 35160 µm microheater length

iii. Current density vs. microbridges lengths.

Similar to operating temperature and power consumption, current density decreases as the heater length increases. Similar trend for the three heaters length has been shown which related current design with micro bridges lengths and voltage applied. A small decrease in the current density as the length of microbridges increased. Otherwise, increasing voltages drive to current density increases as shown in Tables 13, 14, 15 and Figures 14, 15, 16.

Table 13: Current density of heater under different microbridge lengths and applied voltages at 15560 µm microheater length

Voltage (V)	Current density (mA/fm^2) Length(µm)				
	80	90	100	110	120
0.2	0.476	0.474	0.472	0.47	0.468
0.4	0.859	0.846	0.832	0.819	0.807
0.6	1.108	1.074	1.042	1.012	0.984
0.8	1.234	1.179	1.128	1.082	1.039
1.00	1.274	2.01	1.136	1.078	1.025

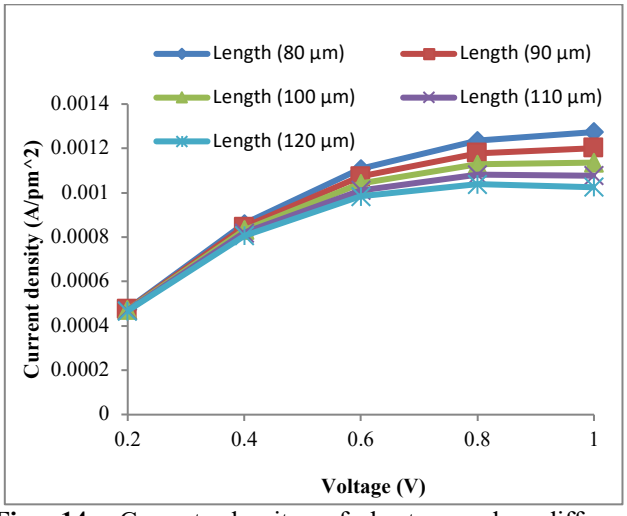

Fig. 14: Current density of heater under different microbridge lengths and applied voltages at 15560 µm microheater length

Table 14: Current density of heater under different microbridge lengths and applied voltages at 24360 µm microheater length

Voltage (V)	Current density (mA/fm^2)				
	Length(µm)				
	80	90	100	110	120
0.2	0.308	0.307	0.307	0.306	0.305
0.4	0.576	0.57	0.564	0.558	0.552
0.6	0.779	0.762	0.746	0.730	0.715
0.8	0.912	0.882	0.853	0.826	0.801
1.00	0.986	0.942	0.902	0.865	0.830

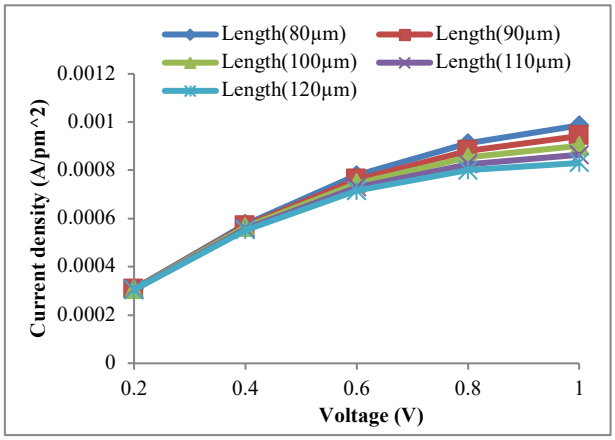

Fig. 15: Current density of heater under different microbridge lengths and applied voltages at 24360 µm microheater length

Table 15: Current density of heater under different microbridge lengths and applied voltages at 35160 µm microheater length

Voltage (V)	Current density (mA/fm^2)				
	Length(µm)				
	80	90	100	110	120
0.2	0.215	0.215	0.214	0.214	0.213
0.4	0.41	0.407	0.404	0.401	0.398
0.6	0.571	0.562	0.553	0.544	0.536
0.8	0.691	0.673	0.657	0.641	0.625
1.00	0.772	0.745	0.72	0.696	0.673

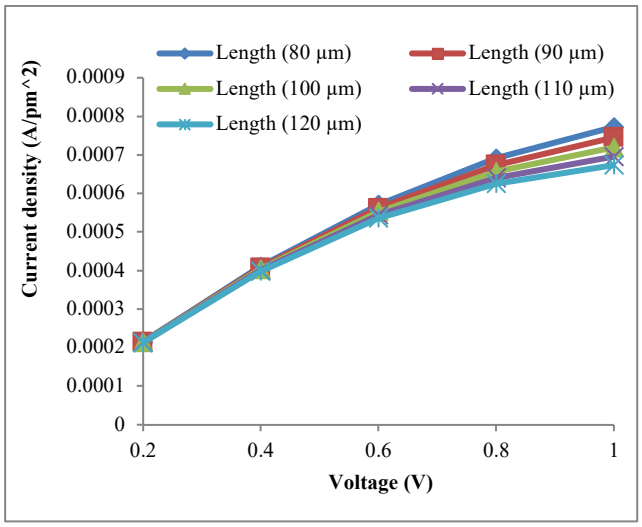

Fig. 16: Current density of heater under different microbridge lengths and applied voltages at 35160 µm microheater length

C. Final specification of the MHP

The final specification of the MHP has been decided based on the analyzed result on the MHP characteristics using mathematical modeling. Table 16 shows the final specification of the layer for the materials at the active area of the MHP. MHP with heater length of 15560 µm and the microbridges with the length 100 µm and width of 25 µm are selected in order to get the desired temperature less than 300 ºC. Where, the device has low power consumption of 3.18 mW with thermal time 7.7 for heating less than 300 ºC, In Li et al. design, the device has a low power consumption of ~19 mW and a rapid thermal response of 8 ms for heating up to 300 ºC [7].

Table 16: Final specifications of the layers materials at the active area of the MHP

Layers	Thickness µm	Width µm	length µm
Si	300	450	450
Sio2	0.56	450	450
Poly	0.56	450	450
Microbridge (1bridge)	0.56	25	100
Heater distributor plate(metal 1&3)	0.56	400	400
Heater	0.56	5	15560
Temperature sensor	0.56	5	800
Interdigited electrode	0.56	5	11600
Passivation layer (Si3N4)	0.56	450	450

5 Conclusions

The designed mathematical model based on the variation of lengths 80 µm and 120 µm and widths 5 µm and 25 µm of microbridge and different lengths of microheater (15560 µm to 35160 µm) under applied voltage from 0.2 V to 1 V were used to determine MHP characteristics. From the obtained results, MHP with heater length of 15560 µm provided the suitable operating temperature that the device needed to be compatible with integrated circuit. From the obtained results, MHP with a heater length of 15560 µm, microbridge length of 100 µm and applied voltages from 0.2 V to 1 V showed a suitable operating temperature from 11.117 ºC to 277.925 ºC with power dissipation from 0.264 mW to 3.181 mW.

References

[1] J. Lee, C. M. Spadaccini, E. V. Mukerjee, and W. P. King, Suspended membrane single crystal silicon micro hotplate for differential scanning calorimetry, in Proc. IEEE 22nd Int. Conf. Micro Electro Mech. Syst., 852–855(2002).

[2] S. Mendoza-Acevedo and M. A. Reyes-Barranca, Study for the micromachining optimization of micro hotplates used in MEMS-CMOS gas sensors, in Proc. 8th Int. Conf. Electr. Eng., Comput. Sci. Autom. Control.,1–6 (2011).

[3] H. Liu, L. Zhang, K. H. H. Li, & O. K. Tan, Microhotplates for metal oxide semiconductor gas sensor applications—towards the CMOS-MEMS monolithic approach, Micromachines., **9(11)**, 557(2018).

[4] M. Gad-el-Hak , The MEMS Handbook, Boca Raton: CRC PRESS., (2002).

[5] J.W. Gardner, P.K. Guha, F. Udrea, J.A. Covington, "CMOS Interfacing for Integrated Gas Sensors: A Review," IEEE Sens. J., **10**, 1833–1848 (2010).

[6] D. Barrettino, M. Graf, M. Zimmermann, C. Hagleitner, A. Hierlemann, H. Baltes, "A smart single-chipmicro-hotplate-based gas sensor system in CMOS-technology". Analog Integr. Circuits Signal Process., **39**, 275–287 (2004).

[7] Y. Li, J. Yu, H. Wu and Z. Tang, Design and fabrication of a CMOS-compatible MHP gas sensor. AIP Advances., **4(3)**, 031339, (2014).

[8] W. Z. Liao, C. L. Dai and M. Z. Yang, Micro ethanol sensors with a heater fabricated using the commercial 0.18 µm CMOS process, Sensors.,**13(10)**., 12760-12770 (2013).

[9] M. Z. Yang, and C. L. Dai, Ethanol microsensors with a readout circuit manufactured using the CMOS-MEMS technique, Sensors, **15(1)**, 1623-1634 (2015).

[10]R. Phatthanakun, P. Deekla, W. Pummara, C. Sriphung, C. Pantong, and N. Chomnawang, Design and fabrication of thin-film aluminum microheater and nickel temperature sensor, 7th IEEE Int. Conf. Nano., (2012).

[11] L. Filipovic, S. Selberherr, "Thermo-electro-mechanical simulation of semiconductor metal oxide gas sensors," Materials., 12(15), 2410 (2019).